石井賢二	アルツハイマー病患者と健常者における アミロイドイメージング	Cognition and Dementia	9(4)	293-300	2010
石井賢二	アルツハイマー病研究におけるアミロイドPET	BRAIN and NERVE	62(7)	757-767	2010
石井賢二	アルツハイマー病-update　臨床検査SPECT, PET	Clinical Neuroscience	28(9)	1015-1017	2010
石井賢二	日本でのアルツハイマー病研究の動き～J-ADNIにおけるPET検査の重要性と今後の展望～	Medical Now	67	6-9	2010
石井賢二	PETによるアミロイドイメージングを用いたAD診断	Med Imag Tech	28(1)	26-30	2010
篠遠 仁	認知症でみられる非認知症状とその対応. 3)代表的な身体合併症	神経内科	72 [Suppl.6]	151-156	2010
島田斉, 樋口真人	アミロイドとミクログリアの画像化	Frontiers in Parkinson Disease	第3巻 第4号	32-35	2010
島田斉, 伊藤彰一	Voxel-based morphometry	Clinical Neuroscience	28	527-530	2010
伊藤健吾, 加藤隆司	Alzheimer病　6）画像診断－PETによる早期および鑑別診断のエビデンスと臨床研究－	神経内科	72	290-295	2010
伊藤健吾, 加藤隆司	アルツハイマー病のFDG PETコホートの現状	PETジャーナル	11	32-34	2010
石井賢二	認知症の新しい画像診断法	Modern Physician	30(1)	58-61	2010
石井賢二	[^{11}C]フルマゼニルによるGABAA受容体 PETイメージング	RADIOISOTOPES	59(1)	49-58	2010
篠遠 仁	認知症の診断-この10年とこれから - 機能画像の進歩	老年精神	21	42-48	2010
石井賢二	軽度認知障害の画像診断	老年精神医学雑誌	20(3)	271-279	2009
篠遠 仁	PET, SPECT -パーキンソン病における 治療効果の評価-	日本臨床	67	228-232	2009
篠遠 仁	アミロイドイメージングの進歩	Clinician	56	44-50	2009
伊藤健吾, 加藤隆司	FDG-PETによるアルツハイマー病の早期診断	Dementia Japan	23	14-21	2009
伊藤健吾, 加藤隆司	認知症の診断と根本治療薬の開発に貢献する PETイメージング	日本神経精神薬理雑誌	29	153-160	2009
石井賢二	ポジトロン断層法（PET）の現状と展望	Medical Technology	37(3)	241-247	2009
石井賢二	MCIの画像診断を考える -PIB-PETによる画像診断の将来-	老年精神医学雑誌	20(増刊号-I)	55-60	2009
石井賢二	アミロイドイメージング	Clinical Neuroscience	27(1)	108-109	2009
加藤隆司, 籏野健太郎, 伊藤健吾	認知症診療における核医学の進歩と課題-アミロイドイメージング-特集 核医学の最前線	映像情報Medical	40	976-979	2008

6. 邦文単行本

著者名	論文題名	書名	編集者名	出版社名	出版地	頁	出版年
石井賢二	アルツハイマー病の発症はアミロイドイメージングでどこまで予測できるか?	EBM精神疾患の治療2011-2012	上島国利, 三村將, 中込和幸, 平島奈津子	中外医学社	東京	241-246	2011
石井賢二	診断薬と診断補助薬, 診断用機器 ～脳アミロイド診断薬～	新薬展望2011（医薬ジャーナル増刊号）		医薬ジャーナル社	大阪	403-408	2011

石井賢二	アミロイドPET画像で診るアルツハイマー病	見て診て学ぶ認知症の画像診断.改訂第2版	松田博史，朝田隆	永井書店	東京	179-189	2010
石井賢二	認知症	臨床医とコメディカルのための最新クリニカルPET	米倉義晴ほか	先端医療技術研究所	東京	179-183	2010
石井賢二	認知症の画像所見　SPECT･PET	最新医学・別冊 新しい診断と治療のABC 66 認知症	三村将	最新医学社	東京	170-178	2010
篠遠 仁	アセチルコリンエステラーゼイメージング	見て診て学ぶ認知症の画像診断.改訂第2版	松田博史，朝田隆	永井書店	大阪	380-390	2010
石井賢二	アミロイドイメージング	Annual Review神経2010	鈴木則弘ほか	中外医学社	東京	57-64	2010
篠遠 仁	Alzheimer病の分子イメージング	Annual Review神経2008	柳澤信夫，篠原幸人，岩田　誠，清水輝夫，寺本　明	中外医学社	東京	35-43	2008
尾内康臣	PET	アルツハイマー病		日本臨床社	東京	282-287	2008
百瀬敏光	Alzheimer病の早期画像診断-発症前診断を目指して-	医学のあゆみ 別冊 老化と疾患	大内尉義	医歯薬出版株式会社	東京	47－51	2008
細川大雅，百瀬敏光	アルツハイマー型認知症　精神疾患の脳画像解析・診断学	老化と疾患　病態の理解と診断・治療の進歩	平安良雄，笠井清登	南山堂	東京	107-109	2008

IV. 研究成果の刊行物・別刷

Neurol Sci
DOI 10.1007/s10072-011-0479-6

CASE REPORT

Two cases of dementias with motor neuron disease evaluated by Pittsburgh compound B-positron emission tomography

Yoshihiro Yamakawa · Hiroyuki Shimada · Suzuka Ataka · Akiko Tamura · Hideki Masaki · Hiroshi Naka · Tsuyoshi Tsutada · Aki Nakanishi · Susumu Shiomi · Yasuyoshi Watanabe · Takami Miki

Received: 1 August 2010 / Accepted: 11 January 2011

Abstract We described the cases of two patients with dementia associated with motor neuron disease, the former with frontotemporal dementia (FTD) and the latter with Alzheimer's disease (AD), studied by the Pittsburgh compound B-positron emission tomography (PIB-PET). In the FTD patient, the PIB-PET revealed no amyloid accumulation in the cortex, whilst in the AD patient showed amyloid accumulation mainly in the frontal, parietal and lateral temporal lobes, besides the posterior cingulate gyrus and the precuneus. Thus, PIB-PET might facilitate the discrimination of different proteinopathies that cause neurodegenerative diseases, as dementia associated with ALS.

Keywords Pittsburgh compound B (PIB) · Amyotrophic lateral sclerosis · Alzheimer disease · Frontotemporal dementia · Motor neuron disease

Y. Yamakawa · H. Shimada (✉) · S. Ataka · A. Tamura · H. Naka · T. Tsutada · T. Miki
Department of Geriatric Medicine and Neurology, Osaka City University Graduate School of Medicine, 1-4-3 Asahi-machi, Abeno-ku, Osaka 545-8586, Japan
e-mail: h.shimada@med.osaka-cu.ac.jp

S. Shiomi
Department of Nuclear Medicine, Osaka City University Graduate School of Medicine, Osaka, Japan

H. Masaki · A. Nakanishi
Kosai-in Hospital, Osaka, Japan

Y. Watanabe
RIKEN Center for Molecular Imaging Science, Kobe, Japan

Y. Watanabe
Department of Physiology, Osaka City University Graduate School of Medicine, Osaka, Japan

Published online: 05 February 2011

Introduction

Some motor neuron diseases (MNDs) are accompanied by cognitive impairment and occasionally confused with Alzheimer's disease (AD). Frontotemporal dementia (FTD) can occur clinically in patients with MND in approximately 2% of sporadic amyotrophic lateral sclerosis (ALS) cases; this condition is called as FTD-MND [1]. On the other hand, some studies suggest that from one-third to half of the ALS patients have some types of cognitive impairments, including AD, throughout the clinical course, and many studies have indicated an overlap between ALS and cognitive impairment [2].

It has been reported that FDG-PET is useful for the differential diagnosis of several types of dementia, especially AD and FTD. Recently, Pittsburgh compound B-positron emission tomography (PIB-PET) has been used to evaluate the degree of amyloid accumulation in the brain. In general, AD is characterized by the accumulation of amyloid in the cortex of the frontal, parietal, and lateral temporal lobes, whereas this type of accumulation is not specific for FTD. Therefore, the evaluation of the cortex using PIB-PET could help us to understand the origin of the cognitive impairment.

We conducted PIB-PET study in two cases of dementia associated with MND to confirm the clinical significance of the PET study.

Case report

Case report 1

A 61-year-old man presented with cognitive impairment with muscle atrophy and muscle weakness of the first

dorsal interosseus; the condition had been progressive since October 2007. On admission to our hospital in 2008, the score for Hasegawa's Dementia Scale-Revised (HDS-R) was 11/30, and that for Mini-Mental State Examination (MMSE) was 15/30, in which recent memory, verbal recall, and orientation were mainly affected. Frontal signs such as forced laughter, personality disorder, and depressive mood were also observed. In addition, atrophy of the tongue, fasciculations in the thigh, and weaknesses of the distal muscles of the upper limbs, mainly in the first dorsal interosseus were observed. Jaw and knee reflexes were hyperactive, and both snout and tonic planter reflexes were present. However, sensory deficits were not detected. His medical history was unremarkable, and he had no family history of neurological diseases. He was diagnosed as the clinically probable ALS with the El-Escorial criteria [3] and refused the treatment with riluzole and had no treatment. Nerve conduction studies (NCS) were normal, while needle electromyography (EMG) studies showed both spontaneous activities and diffuse neurological changes in the extremities and trunk; these symptoms were compatible with MND. Magnetic resonance imaging (MRI) showed mild atrophy in both the frontal and parietal lobes and in the left hippocampus (Fig. 1). PIB-PET indicated no accumulation of amyloids in the cortex, while PET with 18F-fluorodeoxyglucose (FDG-PET) indicated depressed metabolism of glucose in the frontal and temporal lobes (Fig. 2); these signs were compatible with FTD. These findings suggested that the patient had FTD-MND.

Case report 2

A 79-year-old woman presented with cognitive impairment which had been progressive since September 2005. She developed bulbar palsy, including dysarthria and dysphagia, since December 2007 and March 2008, respectively. Initial evaluation in 2005 revealed that her HDS-R score was 25/30 and MMSE score was 25/30. The neurologic examination was normal. The diagnosis was mild cognitive impairment and, after 3 years, HDS-R was 21/30 and MMSE was 24/30, with disturbances in both recent memory and orientation. Atrophy and fasciculation of the tongue were observed, while mild muscle atrophy and weakness of the neck and both the upper limbs were observed. Deep tendon reflexes in both the upper limbs were hyperactive, and snout reflex was present. However, there were no sensory deficits. Her medical history was unremarkable, and she had no family history of neurological diseases. NCS were normal, whereas needle EMG studies revealed high amplitude, long duration, and polyphasic spontaneous activities in the upper extremities, although spontaneous activities were not found. These findings suggest that this patient was compatible to the clinically probable laboratory- supported ALS with the El-Escorial criteria [3] with the one lesion showed the upper and lower motor signs. Brain MRI showed mild atrophy in both the left and right hippocampus and diffuse atrophy in the cerebral cortex consistent with her age (Fig. 3). PIB-PET indicated accumulation of amyloids mainly in the frontal lobe, anterior

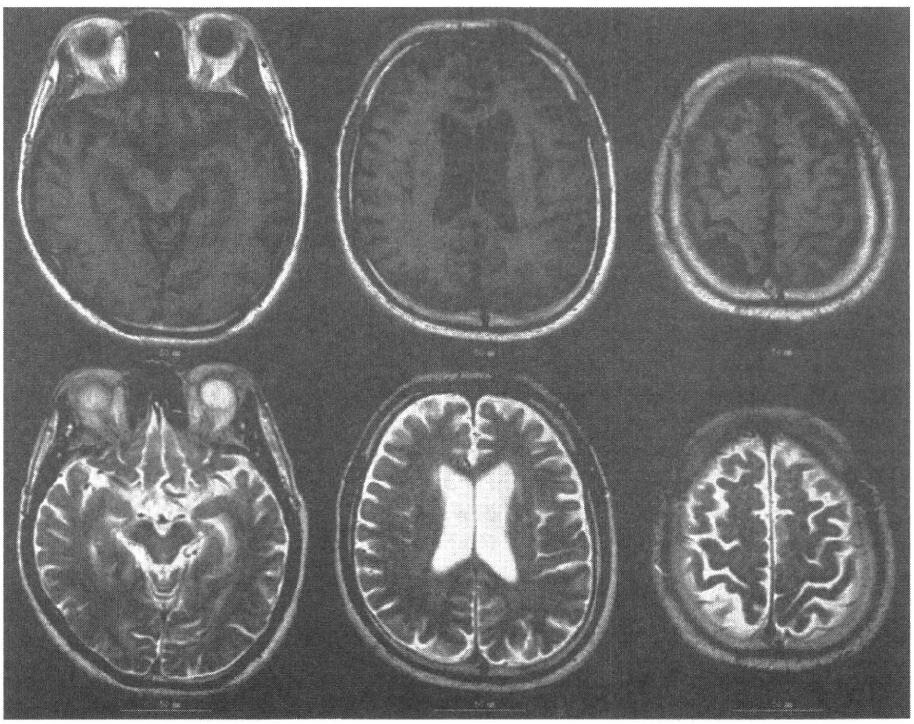

Fig. 1 Mild atrophy of both the frontal and parietal lobes and the left medial temporal area

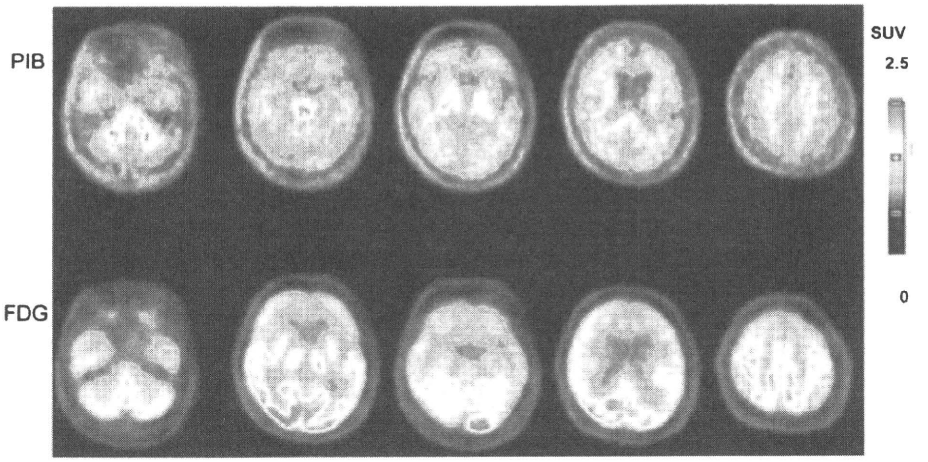

Fig. 2 *Upper panel* PIB-PET shows no accumulation of amyloids in the cortex. *Lower panel* FDG-PET shows decreased glucose metabolism in the frontal and temporal lobes with left-side dominancy associated with decreased metabolism in the right cerebellar hemisphere

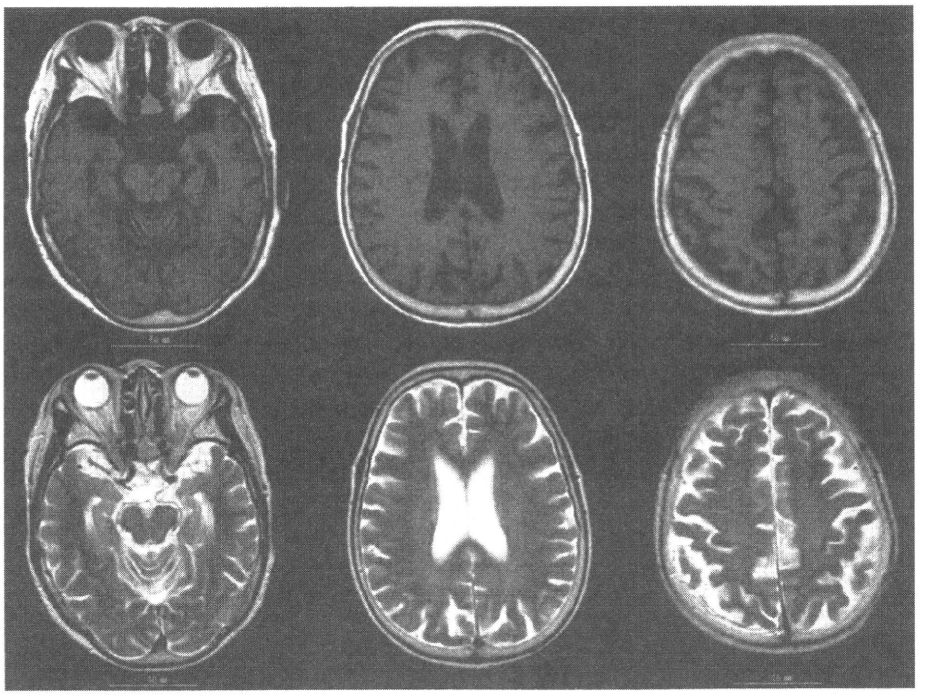

Fig. 3 Atrophy of bilateral medial temporal areas. Age-associated diffuse atrophy of the cerebral cortex

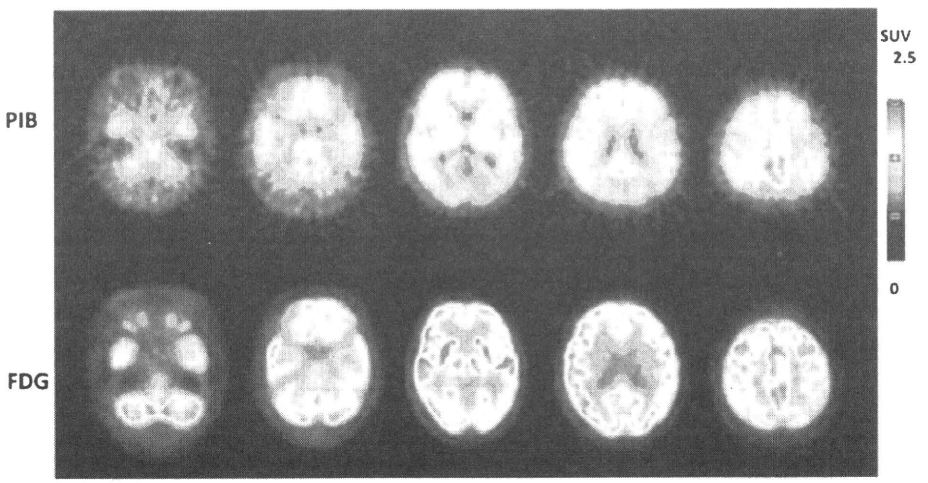

Fig. 4 *Upper panel* PIB-PET shows accumulation of amyloids mainly in the frontal lobe, anterior and posterior cingulate gyrus, precuneus, and also in the parietal lobe and lateral temporal lobe. *Lower panel* FDG-PET shows decreased glucose metabolism in bilateral parietal lobes with left-side dominancy and left lateral temporal lobe [15–23]

Table.1 Previous and present cases of motor neuron disease associated with dementia

	Tsuchiya et al. [15] 1	Ishihara K et al. [16]	Tsuchiya et al. [17] 2	Yokota O et al. [18]	Yamamoto et al. [19]	Yamamoto et al. [19]	Matsuda et al. [20]	Osoegawa et al. [21]	Yamashita et al. [22]	Rusina et al. [23]	Rusina et al. [23]	Present case 1	Present case 2
Clinical features													
Age of onset (years)	69	52	30	48	51	64	65	56	72	68	62	61	79
Age of emergence of dementia (years)	70	52	30	48	51	64	67	58	73	69	62	61	79
Age of emergence of motor neuron disease (years)	69	52	44	53	54	64	67	56	72	68	62	61	81
Duration (years)	2	7	15	6	4	4	3	4	1.5	20 months	2		
Sex	Female	Female	Female	Female	Male	Female	Male	Male	Female	Female	Male	Male	Female
Initial symptoms	Dysarthria and gait disturbance	Speech difficulties	Abnormal behavior	Abnormal behavior	Personality change	Personality change	Motor aphasia	Muscle weakness	Bulbar palsy	Bulbar palsy and motor impairment	Bulbar palsy and cognitive impairment	Cognitive impairment, muscle atrophy, and muscle weakness	Cognitive impairment
Prominent symptoms	Bulbar palsy and gait disturbance	Bulbar palsy	Bulbar palsy	Bulbar palsy and gait disturbance	Bulbar palsy	Bulbar palsy and gait disturbance	Bulbar palsy	Muscle atrophy and muscle weakness	Bulbar palsy	Muscle weakness	Muscle weakness	Muscle atrophy and muscle weakness	Bulbar palsy
Upper motor neuron signs	(+)	(+)	(+)	(+)	(+)	(+)	(+)	(−)	(+)	(+)	(+)	(+)	(+)
Family history	(−)	(−)	(−)	(−)	(−)	(−)	(−)	(−)	Unknown	(−)	(−)	(−)	(−)
Part of brain atrophy													
Frontal lobe	(−)	(−)	(+)	Unknown	Bilateral	Bilateral	Bilateral					Bilateral	(−)
Temporal lobe	Right	(−)	(+)	Unknown	Bilateral	Right	Bilateral					(−)	(−)
Caudate nucleus	(−)	(+)	(+)	Unknown	(−)	(−)	(−)					(−)	(−)
Hippocampus	(−)	(−)	(−)	(−)	(−)	(−)	(−)					Left	(+)
Histological features													
Tau pathology	(−)	(−)	(−)	Neurofibrillary tangles in the frontal and temporal lobe	(−)	(−)							
Ubiquitin-positive inclusions	(+)	(−)	(+)	(−)	(+)	(+)							
Diagnosis	FTD-MND	FTLD associated with MND	†FTD-MND	‡FTLD associated with §MND	FTD-MND	FTD-MND	FTD-MND	Alzheimer's disease with FTD-MND	Alzheimer's disease associated with MND	Alzheimer's disease associated with MND	Alzheimer's disease associated with MND	FTD-MND	Alzheimer's disease associated with MND

† *FTD-MND* frontotemporal dementia with motor neuron disease, ‡ *FTLD* frontotemporal lobar degeneration, § *MND* motor neuron disease

and posterior cingulate gyrus, precuneus, and also in the parietal and lateral temporal lobes. FDG-PET indicated depressed metabolism of glucose in both the parietal lobes and in the left lateral temporal lobe (Fig. 4). These findings suggested that the patient had AD since 2005, and had slowly progressive MND since 2007.

Discussion

The novel PET tracer ^{11}C-PIB has a high affinity for fibrillar amyloid beta protein (Aβ). Klunk W et al. [4] reported that the in vitro 2-(4′-methylaminophenyl) benzothiazole (BTA-1) binding was over tenfold higher in the AD brain than in the normal brain, and that the majority (94%) of the binding was specific for amyloid, and high-affinity BTA-1 was observed only in the AD brain gray matter. However, Aβ accumulation is one of the pathologic hallmarks of AD, but not of frontotemporal lobar degeneration (FTLD), as shown in the criteria proposed by McKhann et al. [1] in 2001; according to the criteria, FTLD is classified into three major groups depending on the presence or the absence of tauopathy and ubiquitinopathy. Alternatively, according to the criteria proposed by Cairns et al. [5] in 2007, FTLD is classified in terms of the presence or the absence of the 43-kDa transactive response (TAR) DNA-binding protein (TDP-43 or TARDBP), which was identified by Arai T et al. [6]. ^{11}C-PIB binds specifically to fibrillar Aβ in AD brains, but shows a low binding affinity to brains from patients with non-Aβ dementias, including FTLD. PIB-PET demonstrated significantly higher ^{11}C-PIB retention in the gray matter of AD patients than that of FTLD patient [7]. In a previous study conducted on 30 ALS patients, 50% had Aβ plaques at histopathological examination; however, of the seven cases without cortical motor neuron inclusions, only two had neuritic plaques [8].

Table 1 summarizes previous and present cases of MND associated with dementia. In 7 of the 8 cases of FTLD associated with MND, including FTD-MND, the age of onset ranged from the half of the fifth to the half of the sixth decade of life, as in our case 1. The mean age of onset of FTLD with MND was 55.6 $\pm$ 15.9 years, whereas that associated with MND varied around 50 years. About the cognitive features, most patients with FTD/ALS show almost the same cognitive and behavioural impairments of FTD patients.

There are some cases where the clinical course of FTD is similar to that of AD, and vice versa; hence, clinical course is not helpful in confirming the diagnosis. Reñé et al. [9] reported that MRI showed frontal and/or temporal atrophy in 62% of the FTLD cases, and single-photon emission computed tomography (SPECT) showed frontal and/or temporal hypoperfusion in 75% of the FTLD cases. It has been reported that FDG-PET is useful in the differential diagnosis of AD from FTLD with more than 85% sensitivity and specificity [10]. Recently, Zhou [11] reported the efficacy of the differential diagnosis of AD from variant form of FTD with the resting state functional magnetic response imaging (RS-fMRI). On the other hand, the accumulation of amyloids is observed in AD but not in FTLD. Our study showed that AD associated with ALS showed positive PIB scans, whereas FTD-MND showed negative scans. In some cases, neither the clinical course nor radiological analyses other than functional neuroimaging techniques are useful in discriminating AD from FTD, especially in the initial stage of the disease.

Recently, the TDP-43 protein has been identified as the cause of FTD/ALS [6] and the mutation of SOD1 gene has been already reported as the cause of familial ALS [12]. Some mutations of the TDP-43 gene may contribute significantly to the aggregation and forming amyloid structures inducted by the C-terminal fragments of the TDP-43 [13]. On the other hand, the SOD1 mutant increased aggregation propensity and formation of amyloid like fibrils [14]. Because these studies suggest that their mutation affect the amyloid formation in the brain of the FTLD patients, we have to consider the possibilities of these mutations affect to our PET data. In the future, we would like to analyze the presence of these mutations of our patients' gene.

Our study suggests that PIB-PET can be considered as a useful tool to discriminate the different proteinopathies that cause neurodegenerative diseases, as dementia associated with ALS.

References

1. McKhann GM, Albert MS, Grossman M, Miller B, Dickson D, Trojanowski JQ (2001) Clinical and pathological diagnosis of frontotemporal dementia: report of the work group on frontotemporal dementia and Pick's disease. Arch Neurol 58(11): 1803–1809. doi:nsa10000
2. Ringholz GM, Appel SH, Bradshaw M, Cooke NA, Mosnik DM, Schulz PE (2005) Prevalence and patterns of cognitive impairment in sporadic ALS. Neurology 65(4):586–590. doi:10.1212/01.wnl.0000172911.39167.b6
3. Brooks BR, Miller RG, Swash M, Munsat TL (2000) El Escorial revisited: revised criteria for the diagnosis of amyotrophic lateral sclerosis. Amyotroph Lateral Scler Other Motor Neuron Disord 1(5):293–299
4. Klunk WE, Wang Y, Huang GF, Debnath ML, Holt DP, Shao L, Hamilton RL, Ikonomovic MD, DeKosky ST, Mathis CA (2003) The binding of 2-(4'-methylaminophenyl)benzothiazole to postmortem brain homogenates is dominated by the amyloid component. J Neurosci 23(6):2086–2092. doi:23/6/2086
5. Cairns NJ, Bigio EH, Mackenzie IR, Neumann M, Lee VM, Hatanpaa KJ, White CL 3rd, Schneider JA, Grinberg LT,

Halliday G, Duyckaerts C, Lowe JS, Holm IE, Tolnay M, Okamoto K, Yokoo H, Murayama S, Woulfe J, Munoz DG, Dickson DW, Ince PG, Trojanowski JQ, Mann DM (2007) Neuropathologic diagnostic and nosologic criteria for frontotemporal lobar degeneration: consensus of the consortium for frontotemporal lobar degeneration. Acta Neuropathol 114(1):5–22. doi:10.1007/s00401-007-0237-2

6. Arai T, Hasegawa M, Akiyama H, Ikeda K, Nonaka T, Mori H, Mann D, Tsuchiya K, Yoshida M, Hashizume Y, Oda T (2006) TDP-43 is a component of ubiquitin-positive tau-negative inclusions in frontotemporal lobar degeneration and amyotrophic lateral sclerosis. Biochem Biophys Res Commun 351(3):602–611. doi:10.1016/j.bbrc.2006.10.093
7. Rabinovici GD, Furst AJ, O'Neil JP, Racine CA, Mormino EC, Baker SL, Chetty S, Patel P, Pagliaro TA, Klunk WE, Mathis CA, Rosen HJ, Miller BL, Jagust WJ (2007) 11C-PIB PET imaging in Alzheimer disease and frontotemporal lobar degeneration. Neurology 68(15):1205–1212. doi:10.1212/01.wnl.0000259035.98480.ed
8. Hamilton RL, Bowser R (2004) Alzheimer disease pathology in amyotrophic lateral sclerosis. Acta Neuropathol 107(6):515–522. doi:10.1007/s00401-004-0843-1
9. Rene R, Campdelacreu J, Escrig A, Gascon-Bayarri J, Hernandez-Pardo M, Jauma S, Rubio F (2008) Frontotemporal lobar degeneration: a descriptive study of 42 patients. Neurologia 23(8):511–517. doi:20081090816
10. Mosconi L, Tsui WH, Herholz K, Pupi A, Drzezga A, Lucignani G, Reiman EM, Holthoff V, Kalbe E, Sorbi S, Diehl-Schmid J, Perneczky R, Clerici F, Caselli R, Beuthien-Baumann B, Kurz A, Minoshima S, de Leon MJ (2008) Multicenter standardized 18F-FDG PET diagnosis of mild cognitive impairment, Alzheimer's disease, and other dementias. J Nucl Med 49(3):390–398. doi:10.2967/jnumed.107.045385
11. Zhou J, Greicius MD, Gennatas ED, Growdon ME, Jang JY, Rabinovici GD, Kramer JH, Weiner M, Miller BL, Seeley WW Divergent network connectivity changes in behavioural variant frontotemporal dementia and Alzheimer's disease. Brain 133 (Pt 5):1352–367. doi:awq075 [pii] 10.1093/brain/awq075
12. Orrell R, de Belleroche J, Marklund S, Bowe F, Hallewell R (1995) A novel SOD mutant and ALS. Nature 374(6522):504–505. doi:10.1038/374504a0
13. Chen AK, Lin RY, Hsieh EZ, Tu PH, Chen RP, Liao TY, Chen W, Wang CH, Huang JJ Induction of amyloid fibrils by the C-terminal fragments of TDP-43 in amyotrophic lateral sclerosis. J Am Chem Soc 132 (4):1186–187. doi:10.1021/ja9066207
14. Yoon EJ, Park HJ, Kim GY, Cho HM, Choi JH, Park HY, Jang JY, Rhim HS, Kang SM (2009) Intracellular amyloid beta interacts with SOD1 and impairs the enzymatic activity of SOD1: implications for the pathogenesis of amyotrophic lateral sclerosis. Exp Mol Med 41(9):611–617. doi:10.3858/emm.2009.41.9.067
15. Tsuchiya K, Ikeda K, Haga C, Kobayashi T, Morimatsu Y, Nakano I, Matsushita M (2001) Atypical amyotrophic lateral sclerosis with dementia mimicking frontal Pick's disease: a report of an autopsy case with a clinical course of 15 years. Acta Neuropathol 101(6):625–630
16. Ishihara K, Araki S, Ihori N, Shiota J, Kawamura M, Nakano I (2006) An autopsy case of frontotemporal dementia with severe dysarthria and motor neuron disease showing numerous basophilic inclusions. Neuropathology 26(5):447–454
17. Tsuchiya K, Takahashi M, Shiotsu H, Akiyama H, Haga C, Watabiki S, Taki K, Nakano I, Ikeda K (2002) Sporadic amyotrophic lateral sclerosis with circumscribed temporal atrophy: a report of an autopsy case without dementia and with ubiquitinated intraneuronal inclusions. Neuropathology 22(4):308–316
18. Yokota O, Tsuchiya K, Oda T, Ishihara T, de Silva R, Lees AJ, Arai T, Uchihara T, Ishizu H, Kuroda S, Akiyama H (2006) Amyotrophic lateral sclerosis with dementia: an autopsy case showing many Bunina bodies, tau-positive neuronal and astrocytic plaque-like pathologies, and pallido-nigral degeneration. Acta Neuropathol 112(5):633–645. doi:10.1007/s00401-006-0141-1
19. Yamamoto R, Iseki E, Murayama N, Minegishi M, Kimura M, Eto K, Arai H, Ohbu S, Hatanaka D, Hino H, Fujisawa K (2007) Clinico-pathological investigation of two patients with dementia with motor neuron disease. Brain Nerve 59(3):263–269
20. Matsuda M, Miki J, Hattori T, Tabata K (2000) A case of motor neuron disease with dementia, presenting motor aphasia as an initial symptom. Rinsho Shinkeigaku 40(2):160–165
21. Osoegawa M, Takao T, Taniwaki T, Kikuchi H, Arakawa K, Furuya H, Iwaki T, Kira J (2001) An autopsy case of dementia with motor neuron disease accompanying Alzheimer's disease lesion. Rinsho Shinkeigaku 41(8):482–486
22. Yamashita M, Yamamoto T, Nakamura (1997) Concurrence of amyotrophic lateral sclerosis with limbic degeneration and Alzheimer's disease. Neuropathology 17:334–339
23. Rusina R, Sheardova K, Rektorova I, Ridzon P, Kulist'ak P, Matej R (2007) Amyotrophic lateral sclerosis and Alzheimer's disease—clinical and neuropathological considerations in two cases. Eur J Neurol 14(7):815–818. doi:10.1111/j.1468-1331.2007.01759.x

J Neurol
DOI 10.1007/s00415-009-5377-y

LETTER TO THE EDITORS

Posterior cortical atrophy with [^{11}C] Pittsburgh compound B accumulation in the primary visual cortex

Taiki Kambe · Yumiko Motoi · Kenji Ishii · Nobutaka Hattori

Received: 24 August 2009 / Revised: 24 October 2009 / Accepted: 30 October 2009

Sirs,

Posterior cortical atrophy (PCA) is a presenile dementia that presents primarily with signs and symptoms of cortical visual dysfunction [1]. The most common associated pathologic findings of PCA are amyloid plaques and neurofibrillary tangles predominantly affecting the visual association areas [8]. Although [^{11}C] Pittsburgh compound B (PIB) PET studies of amnestic Alzheimer's disease (AD) have been conducted [2, 3, 5], the link between amyloid-β (Aβ) and regional brain dysfunction remains controversial. However, two PIB studies of PCA supported the possible link between Aβ deposition and clinical features [7, 10]. Here, we describe a patient with PCA who showed left homonymous hemianopsia and uncoupling between PIB uptake and glucose metabolism in the right occipital lobe.

A 63-year-old woman consulted our hospital with a 5-year history of poor vision. She first noticed that characters on posters appeared to be shaking. One year later, she found difficulty in reading subtitles in movies and then she became unable to read books. On neurological examination, she showed left homonymous hemianopsia. A Goldmann dynamic visual field examination demonstrated macular-sparing left homonymous hemianopsia. Visual acuity was normal and bilateral light reflexes were prompt. Other neurological examinations were normal. On neuropsychological evaluations, she showed visuospatial dysfunction and dyscalculia. MMSE score was 26 of 30. Memory function was preserved. She demonstrated disturbed recognition of superimposed figures. Face and color recognition were normal.

Cerebrospinal fluid (CSF) Aβ_{42} was decreased (297 pg/ml) and in normal controls, the levels are 874 $\pm$ 293 pg/ml (mean $\pm$ SD, INNOTEST® β-AMYLOID$_{(1\text{-}42)}$, Innogenetics, Ghent, Belgium). CSF tau protein phosphorylated at serine 199 was increased (1.36 pM). In normal controls, these levels are 0.6 $\pm$ 0.4 pM [4]. [^{18}F] fluorodeoxyglucose (FDG) PET image was acquired for 6 min starting 45 min after the injection of 150 MBq of tracer. The accumulation of [^{11}C] PIB was evaluated by a standardized uptake value ratio (SUVR) on a summing image obtained 40–60 min after injection of 500 MBq of tracer taking the cerebellar cortex as a reference region. [^{18}F] FDG PET showed hypometabolism in the temporo-parieto-occipital lobe predominantly on the right (Fig. 1d–f). [^{11}C] PIB PET demonstrated increased uptake in the bilateral frontal lobes and parietal and occipital cortices with more intense uptake on the right (Fig. 1g–i). In the right occipital lobe, FDG uptake showed lower metabolism in the lateral occipital cortex (Fig. 1d, e, arrow) than in the calcarine cortex (Fig. 1d, e, arrowhead). In contrast, amyloid imaging demonstrated high PIB uptake in the right calcarine cortex (Fig. 1g, h, arrowhead) while the adjacent lateral occipital cortex showed normal PIB uptake (Fig. 1g, h, arrow).

It was shown that macular sparing occurred when the posterior part of the calcarine cortex was spared in patients with striate cortical disease such as infarction, neoplasm and cerebromalacia, while macular splitting occurred when the occipital pole and operculum were involved [6]. Neuroimaging studies of our patient demonstrated that in the occipital lobe, there were two regions showing different

T. Kambe · Y. Motoi (✉) · N. Hattori
Department of Neurology,
Juntendo University School of Medicine,
2-1-1, Hongo Bunkyo-ku, Tokyo 113-8421, Japan
e-mail: motoi@juntendo.ac.jp

K. Ishii
Positron Medical Center,
Tokyo Metropolitan Institute of Gerontology,
1-1 Nakacho, Itabashi, Tokyo 173-0022, Japan

Published online: 14 November 2009

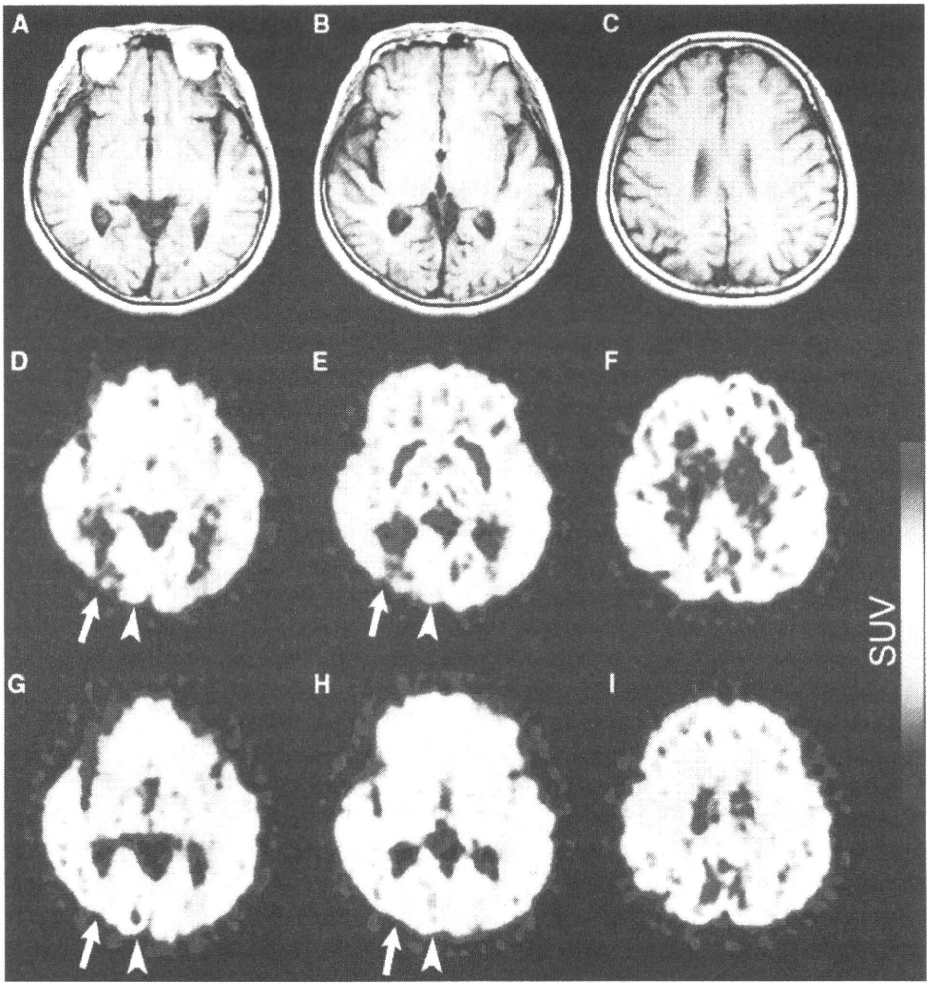

Fig. 1 Transverse T1-weighted MRI sections (**a–c**), PET with [^{18}F] FDG (D-F) and PET with [^{11}C] PIB (**g–i**) of the patient. MRI showed the absence of cerebral infarction and atrophy (**a**). The medial region including the calcarine cortex, (**d**, **e**, **g**, **h** *arrowhead*) showed moderately decreased FDG uptake and very high PIB uptake. In contrast, the lateral region demonstrated severely depressed FDG uptake without remarkable PIB uptake (**d**, **e**, **g**, **h**, *arrow*)

PIB/FDG patterns: a medial region (in the calcarine cortex, Fig. 1d, e, g, h arrowhead) with high PIB uptake and moderately decreased FDG uptake, and a lateral region with normal PIB uptake but severely depressed FDG uptake (Fig. 1d, e, g, h, arrow). Since PIB uptake in the medial region did not spare the occipital pole, we concluded that the lateral region is more likely to have contributed to the macular-sparing left hemianopsia.

We postulate that in the occipital lobe of our patient, Aβ deposition was not associated with the clinical features. Other factors such as neurofibrillary tangles might have contributed to the clinical features [9].

Acknowledgments We are grateful to Dr. Yoko Chikaoka for excellent technique regarding CSF analysis.

References

1. Benson DF, Davis RJ, Snyder BD (1988) Posterior cortical atrophy. Arch Neurol 45:789–793
2. Edison P, Archer HA, Hinz R, Hammers A, Pavese N, Tai YF, Hotton G, Cutler D, Fox N, Kennedy A, Rossor M, Brooks DJ (2007) Amyloid, hypometabolism, and cognition in Alzheimer disease: an [11C]PIB and [18F]FDG PET study. Neurology 68:501–508
3. Frisoni GB, Lorenzi M, Caroli A, Kemppainen N, Nagren K, Rinne JO (2009) In vivo mapping of amyloid toxicity in Alzheimer disease. Neurology 72:1504–1511
4. Itoh N, Arai H, Urakami K, Ishiguro K, Ohno H, Hampel H, Buerger K, Wiltfang J, Otto M, Kretzschmar H, Moeller HJ, Imagawa M, Kohno H, Nakashima K, Kuzuhara S, Sasaki H, Imahori K (2001) Large-scale, multicenter study of cerebrospinal fluid tau protein phosphorylated at serine 199 for the antemortem diagnosis of Alzheimer's disease. Ann Neurol 50:150–156

5. Li Y, Rinne JO, Mosconi L, Pirraglia E, Rusinek H, DeSanti S, Kemppainen N, Nagren K, Kim BC, Tsui W, de Leon MJ (2008) Regional analysis of FDG and PIB-PET images in normal aging, mild cognitive impairment, and Alzheimer's disease. Eur J Nucl Med Mol Imaging 35:2169–2181
6. McFadzean R, Brosnahan D, Hadley D, Mutlukan E (1994) Representation of the visual field in the occipital striate cortex. Br J Ophthalmol 78:185–190
7. Ng SY, Villemagne VL, Masters CL, Rowe CC (2007) Evaluating atypical dementia syndromes using positron emission tomography with carbon 11 labeled Pittsburgh Compound B. Arch Neurol 64:1140–1144
8. Renner JA, Burns JM, Hou CE, McKeel DW Jr, Storandt M, Morris JC (2004) Progressive posterior cortical dysfunction: a clinicopathologic series. Neurology 63:1175–1180
9. Tang-Wai DF, Graff-Radford NR, Boeve BF, Dickson DW, Parisi JE, Crook R, Caselli RJ, Knopman DS, Petersen RC (2004) Clinical, genetic, and neuropathologic characteristics of posterior cortical atrophy. Neurology 63:1168–1174
10. Tenovuo O, Kemppainen N, Aalto S, Nagren K, Rinne JO (2008) Posterior cortical atrophy: a rare form of dementia with in vivo evidence of amyloid-beta accumulation. J Alzheimers Dis 15:351–355

Eur J Nucl Med Mol Imaging (2010) 37:934–941
DOI 10.1007/s00259-009-1314-7

ORIGINAL ARTICLE

In vivo detection of prion amyloid plaques using [^{11}C]BF-227 PET

Nobuyuki Okamura · Yusei Shiga · Shozo Furumoto · Manabu Tashiro · Yoshio Tsuboi · Katsutoshi Furukawa · Kazuhiko Yanai · Ren Iwata · Hiroyuki Arai · Yukitsuka Kudo · Yasuhito Itoyama · Katsumi Doh-ura

Received: 7 August 2009 / Accepted: 21 October 2009 / Published online: 17 December 2009

Abstract
Purpose In vivo detection of pathological prion protein (PrP) in the brain is potentially useful for the diagnosis of transmissible spongiform encephalopathies (TSEs). However, there are no non-invasive ante-mortem means for detection of pathological PrP deposition in the brain. The purpose of this study is to evaluate the amyloid imaging tracer BF-227 with positron emission tomography (PET) for the non-invasive detection of PrP amyloid in the brain.
Methods The binding ability of BF-227 to PrP amyloid was investigated using autoradiography and fluorescence microscopy. Five patients with TSEs, including three patients with Gerstmann-Sträussler-Scheinker disease (GSS) and two patients with sporadic Creutzfeldt-Jakob disease (CJD), underwent [^{11}C]BF-227 PET scans. Results were compared with data from 10 normal controls and 17 patients with Alzheimer's disease (AD). The regional to pons standardized uptake value ratio was calculated as an index of BF-227 retention.
Results Binding of BF-227 to PrP plaques was confirmed using brain samples from autopsy-confirmed GSS cases. In clinical PET study, significantly higher retention of BF-227 was detected in the cerebellum, thalamus and lateral temporal cortex of GSS patients compared to that in the corresponding tissues of normal controls. GSS patients also showed higher retention of BF-227 in the cerebellum, thalamus and medial temporal cortex compared to AD patients. In contrast, the two CJD patients showed no obvious retention of BF-227 in the brain.
Conclusion Although [^{11}C]BF-227 is a non-specific imaging marker of cerebral amyloidosis, it is useful for in vivo detection of PrP plaques in the human brain in GSS, based on the regional distribution of the tracer. PET amyloid imaging might provide a means for both early diagnosis and non-invasive disease monitoring of certain forms of TSEs.

N. Okamura · S. Furumoto · K. Yanai
Department of Pharmacology,
Tohoku University School of Medicine,
Sendai, Japan

Y. Shiga · Y. Itoyama
Department of Neurology,
Tohoku University School of Medicine,
Sendai, Japan

S. Furumoto · R. Iwata
Division of Radiopharmaceutical Chemistry,
Cyclotron and Radioisotope Center, Tohoku University,
Sendai, Japan

M. Tashiro
Division of Cyclotron Nuclear Medicine,
Cyclotron and Radioisotope Center, Tohoku University,
Sendai, Japan

Y. Tsuboi
Department of Neurology,
Fukuoka University School of Medicine,
Fukuoka, Japan

K. Furukawa · H. Arai
Department of Geriatrics and Gerontology,
Division of Brain Sciences, Institute of Development,
Aging, and Cancer, Tohoku University,
Sendai, Japan

Y. Kudo
Innovation of New Biomedical Engineering Center,
Tohoku University,
Sendai, Japan

K. Doh-ura (✉)
Department of Prion Research,
Tohoku University School of Medicine,
2-1 Seiryo-machi, Aoba-ku, Sendai 980-8575, Japan
e-mail: doh-ura@mail.tains.tohoku.ac.jp

Keywords Prion · PET · Amyloid · Creutzfeldt-Jakob disease

Introduction

Transmissible spongiform encephalopathies (TSEs), also known as prion diseases, are a group of fatal neurodegenerative disorders, including Creutzfeldt-Jakob disease (CJD), Gerstmann-Sträussler-Scheinker disease (GSS) and kuru [1–3]. TSEs are characterized by progressive deposition of abnormal prion protein (PrP) in the brain. CJD is the most common type of human TSE and is classified into sporadic, genetic and infectious forms according to the aetiology of illness. GSS is a familial neurodegenerative disorder associated with mutations of the PrP gene and is clinically recognized by cerebellar ataxia combined with postural abnormalities and cognitive decline [1–3]. Two major types of abnormal PrP deposition, synaptic and plaque types, have been described in the brain of people with TSEs [1]. The synaptic type of PrP deposition, which does not have tinctorial properties of amyloid in tissue sections, is most commonly observed in sporadic CJD, whereas the plaque type, which frequently forms congophilic amyloid plaques, is a hallmark of such TSEs as GSS, variant CJD (vCJD) and iatrogenic dura CJD with plaques [1, 4]. Abnormal PrP deposition in the brain is suggested to start before the occurrence of clinical symptoms [5–7]. Thus, preclinical diagnosis and, when available, early disease-specific therapeutic interventions, can be beneficial for people predisposed to or affected by TSEs.

Several positron emission tomography (PET) imaging agents have been recently developed and used for in vivo detection of brain amyloid-β (Aβ) plaques in patients with Alzheimer's disease (AD) [8–12]. Most of these β-sheet binding agents show high binding affinity to PrP amyloid because PrP aggregates in TSEs form β-pleated sheet structures and share a common secondary structure with Aβ deposits in AD brains [13–16]. Therefore, these agents would be useful for the in vivo detection of PrP amyloid in the brain. Two clinical PET studies were performed using [^{18}F]FDDNP and/or [^{11}C]PIB in sporadic and familial CJD patients [17, 18]. The results indicated moderate retention of FDDNP and no obvious retention of PIB in the brain [17, 18]. Therefore, agents that can sensitively detect abnormal PrP deposits should be further explored for the diagnosis of TSEs. We have demonstrated in vitro and in vivo binding of benzoxazole derivatives to both Aβ and PrP amyloids [19, 20]. One of these derivatives, BF-227, was used for a clinical PET study where it successfully visualized amyloid deposits in the brain of AD patients in vivo [12, 21]. Therefore, [^{11}C]BF-227 appears to be a promising candidate for PET imaging of PrP deposits. The purpose of this study was to evaluate the clinical utility of [^{11}C]BF-227 PET for the non-invasive detection of abnormal PrP deposits in patients with TSEs.

Methods

Preparation of compounds

BF-227 and its 2-tosyloxyethoxy and *N*-desmethylated derivatives were custom synthesized by Tanabe R&D Service Co. (Osaka, Japan). [^{18}F]BF-227 was synthesized for autoradiography of brain sections, as described previously [22]. For the clinical studies, [^{11}C]BF-227 was synthesized as described previously [12]. Radiochemical yields were greater than 50% based on [^{11}C]methyl triflate, and specific radioactivities were 119–138 GBq/μmol at the end of synthesis. Radiochemical purities were greater than 95%.

Histopathological staining and in vitro autoradiography

Autopsy-diagnosed brain samples from two GSS cases with PrP plaque deposition and two sporadic CJD cases with synaptic PrP deposition were provided by Dr. Toru Iwaki of the Department of Neuropathology, Kyushu University, Japan. The brain sample from an 81-year-old man with autopsy-confirmed physiological aging was obtained from Tohoku University Hospital. The two GSS cases had a proline-to-leucine mutation at codon 102 and methionine homozygosity at codon 129 of the PrP gene, and the two sporadic CJD cases had no mutations and methionine homozygosity at codon 129; they showed type 1 abnormal PrP in immunoblotting of the brain tissues. All of the brain samples were treated with 98% formic acid for 1 h before paraffin embedding to eliminate prion infectivity. Sections from paraffin-embedded blocks of the cerebellum or frontal cortex were then dewaxed in xylene and ethanol. For staining with BF-227, tissue sections were immersed in 100 μM BF-227 solution containing 50% ethanol for 10 min. They were then dipped briefly into water and rinsed in phosphate-buffered saline for 10 min before coverslipping with FluorSave Reagent (Calbiochem, La Jolla, CA, USA). Subsequently, they were examined using an Eclipse E800 microscope (Nikon, Tokyo, Japan) equipped with a V-2A filter set (excitation, 380–420 nm; dichroic mirror, 430 nm; Longpass filter, 450 nm). For autoradiography, the section was incubated with 1.0 MBq/ml of [^{18}F]BF-227 at room temperature for 10 min and then washed briefly with water and 50% ethanol. After drying, the labelled section was exposed to a BAS-III imaging plate (Fuji Film, Tokyo, Japan) overnight. Autoradiographic images were obtained using a BAS-5000 phosphor imaging instrument (Fuji Film, Tokyo, Japan). Neighbouring sec-

tions were immunostained using 3F4 anti-PrP monoclonal antibody (Covance, Princeton, NJ, USA) as described previously [13, 20].

Subjects and patients in the clinical PET study

Five TSE patients, including two sporadic CJD patients [63-year-old woman (CJD1) and 58-year-old man (CJD2)] and three GSS patients [69-year-old woman (GSS1), 61-year-old man (GSS2) and 30-year-old woman (GSS3)], underwent PET scans with [^{11}C]BF-227 (Table 1). For comparison, [^{11}C]BF-227 PET studies were also performed in 17 AD patients [mean age ± standard deviation (SD)= 72.6±6.7; mean Mini-Mental State Examination score ± SD=19.8±4.0] and 10 aged normal controls (mean age ± SD=67.2±2.5). Some of these AD and normal subjects were included in our previous report [12].

CJD1's health was unremarkable until the manifestation of depressive symptoms at the age of 62 years. The patient then developed subacutely progressive dementia, motor disturbances and myoclonus. CJD2 showed subacutely progressive dementia and gait disturbance and then developed psychotic symptoms, dysarthria and myoclonus. Both CJD patients had no mutations and showed methionine homozygosity at codon 129 of the PrP gene. PET studies in CJD1 and CJD2 were performed when they reached grade 4 of the modified Rankin scale at 3 and 4 months after onset of symptoms, respectively. Both patients showed periodic synchronous discharges in electroencephalograms and hyperintensity in the caudate, putamen and cerebral cortex on diffusion-weighted magnetic resonance (MR) images. Diagnosis of probable CJD was made according to the WHO criteria [23].

Each GSS patient was from a different pedigree and had a family history of the same disease, carrying a proline-to-leucine mutation at codon 102 and methionine homozygosity at codon 129 of the PrP gene. GSS1 and GSS2, having a 9- and 20-month clinical duration from the onset, respectively, showed signs of moderate cerebellar ataxia, such as gait disturbance and slurred speech; however, they could walk unassisted and had slight or no cognitive impairment. GSS1 and GSS2 scored 22 and 26 points, respectively, on the Mini-Mental State Examination. GSS3, having a 27-month clinical duration, showed severe gait disturbance and slurred speech and was unable to walk unassisted; however, she had no cognitive impairment (30 points on the Mini-Mental State Examination) at the time of this study.

AD diagnosis was made according to the National Institute of Neurological and Communicative Diseases and Stroke-Alzheimer's Disease and Related Disorders Association (NINCDS-ADRDA) criteria [24]. CJD, GSS and AD patients were recruited from Miyagi National Hospital, Fukuoka University Hospital, Kagoshima University Hospital and Tohoku University Hospital. Normal controls were recruited from volunteers with no cognitive impairment or cerebrovascular lesions on MR images and who were not taking any centrally acting medications. No significant difference in age distribution was apparent between the groups. This study was approved by the Ethics Committee on clinical investigations of Tohoku University School of Medicine and performed in accordance with the Declaration of Helsinki. Written informed consent was obtained after complete description of the study to the patients and subjects.

Image acquisition protocols

PET scans were performed using a SET-2400W (Shimadzu Inc., Kyoto, Japan). After intravenous injection of 211–366 MBq (5.7–9.9 mCi) of [^{11}C]BF-227, dynamic PET images were obtained for 60 min with the subjects' eyes closed. Arterial blood sampling in the TSE patients was not

Table 1 Regional to pons standardized uptake value ratio (SUVRp) values in aged normal controls (Control), Alzheimer's disease patients (AD), Creutzfeldt-Jakob disease patients (CJD) and Gerstmann-Sträussler-Scheinker disease patients (GSS)

	Control (n=10) Mean ± SD	AD (n=17) Mean ± SD	CJD1	CJD2	GSS (n=3) Mean ± SD	GSS1	GSS2	GSS3
Frontal	0.60±0.03	0.64±0.04	0.57	0.61	0.67±0.08	0.74	0.69	0.57
Lateral temporal	0.59±0.03	0.69±0.04*	0.63	0.62	0.67±0.05*	0.71	0.68	0.61
Parietal	0.62±0.02	0.69±0.04*	0.62	0.62	0.67±0.06	0.72	0.68	0.61
Occipital	0.62±0.04	0.65±0.05	0.62	0.69	0.67±0.07	0.74	0.67	0.60
Medial temporal	0.64±0.04	0.62±0.03	0.57	0.65	0.67±0.02**	0.66	0.70	0.67
Striatum	0.71±0.04	0.75±0.04*	0.69	0.72	0.76±0.04	0.80	0.77	0.72
Thalamus	1.00±0.04	1.01±0.04	0.97	1.04	1.08±0.00*, **	1.08	1.07	1.08
Cerebellum	0.58±0.01	0.57±0.02	0.58	0.59	0.62±0.01*, **	0.61	0.63	0.61

*p<0.05 compared to aged normal group

**p < 0.05 compared to AD group

performed because the Committee on Clinical Investigation at Tohoku University School of Medicine did not approve blood sampling during the PET scan, from the standpoint of infection risk management. T_1-weighted MR images were obtained using a Signa 1.5-T machine (General Electric Inc., Milwaukee, WI, USA).

Image analysis

Standardized uptake value (SUV) images of [^{11}C]BF-227 were obtained by normalizing tissue concentration by injected dose and body weight. Average summations of SUV images were created from early frames (0–30 min post-injection) and late frames (40–60 min post-injection) of dynamic PET images. Early frame images were created for co-registration with individual MR images, and late frame images were used for calculation of SUV. Individual MR images were anatomically co-registered with the early frame PET images using statistical parametric mapping software (SPM2, Welcome Department of Imaging Neuroscience, London, UK) [25]. Spatial normalization was performed using an MR T_1 template of SPM2 to transfer PET images into a standard stereotactic space. Regions of interest (ROIs) were placed on a spatially normalized MR image, as described previously [12]. ROI information was then copied onto delayed PET SUV images, and regional SUV images at 40–60 min post-injection were sampled using Dr.View/LINUX software (AJS, Tokyo, Japan). Deposition of PrP plaques is reportedly frequent in the cerebellum but scarce in the pons of GSS brain [26]. Furthermore, BF-227 retention in the pons does not differ between AD patients and normal controls. Therefore, we used the pons as a reference region and calculated the regional to pons SUV ratio (SUVRp) as an index of BF-227 retention.

Statistical analysis

For statistical comparison in each group, we applied one-way analysis of variance, followed by the Bonferroni-Dunn post hoc test. Statistical comparison of age distribution was performed using the Kruskal-Wallis test, followed by Dunn's multiple comparison test. Statistical significance for each analysis was defined as $p<0.05$.

Results

Autoradiography examination indicated binding of a tracer dose of BF-227 to PrP plaque deposits. BF-227 retention was present in brain sections from GSS cases with PrP plaque deposition but not from normal control cases and sporadic CJD cases with synaptic PrP deposition (Fig. 1a–c). The regional distribution of [^{18}F]BF-227 in the autoradiograms co-localized with the immunostained PrP plaques in the cerebellar cortex of GSS cases (Fig. 1d–e). BF-227 binding to PrP plaques was additionally examined using a microscope, because BF-227 is a fluorescent compound. Core regions of the PrP plaques were intensely stained with BF-227 (Fig. 2, arrows), indicating that BF-227 preferentially binds to the fibril-rich core of PrP amyloid plaques.

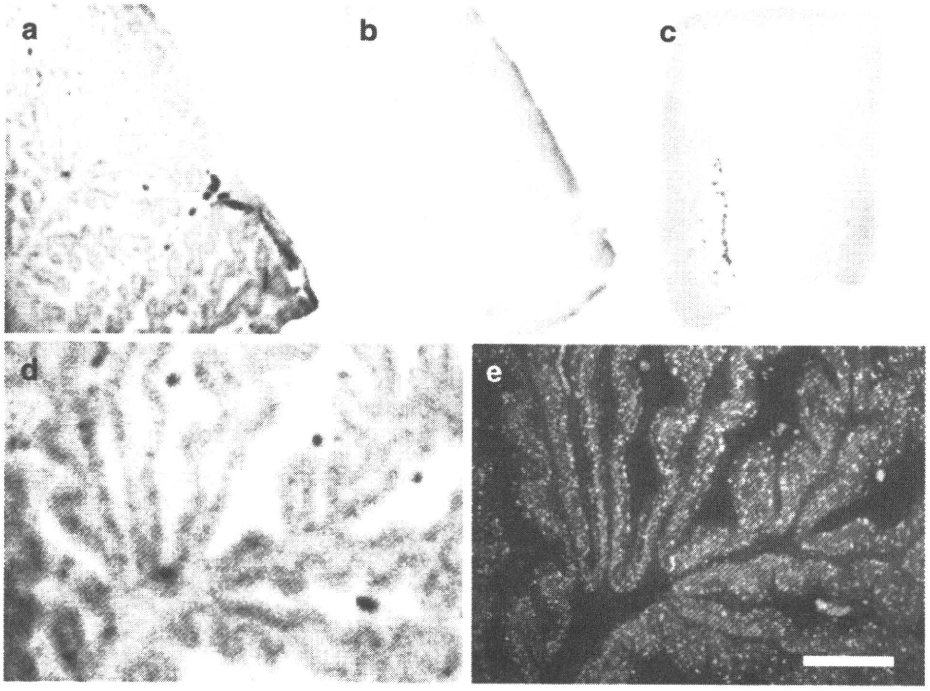

Fig. 1 [^{18}F]BF-227 autoradiograms of a cerebellar section from a Gerstmann-Sträussler-Scheinker (GSS) case (**a**), a cerebellar section from a physiological aging case (**b**) and a frontal cortex section from a sporadic Creutzfeldt-Jakob disease (CJD) case (**c**) are shown, together with a magnified view of **a** (**d**) and prion protein (PrP) immunostaining of the same field as **d** (**e**). BF-227 retention was present in the brain section from a GSS case with PrP plaque deposition, but not from a normal control case and sporadic CJD case with synaptic PrP deposition. *Bar*=200 μm

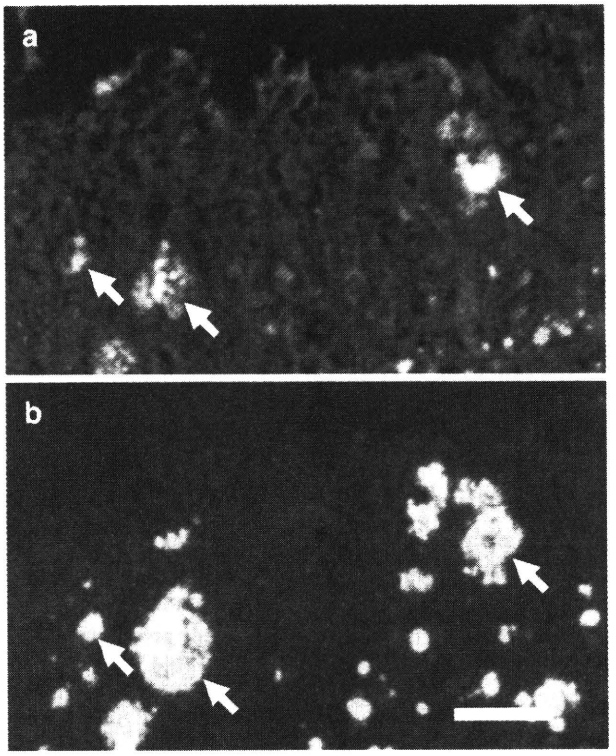

Fig. 2 Microscopic images of BF-227 staining (**a**) and PrP immunostaining (**b**) of the cerebellar cortex of a GSS case. *Arrows* indicate PrP amyloid plaques. The core regions of PrP plaques were intensely stained with BF-227. *Bar*=50 μm

Figure 3 shows the average summations of SUVRp images in an aged normal subject (64-year-old man), a sporadic CJD patient (CJD1, 63-year-old woman), a GSS patient (GSS2, 61-year-old man) and an AD patient (62-year-old woman). As reported previously, non-specific retention of [^{11}C]BF-227 was observed in the brain stem and white matter of all subjects [12]. The GSS patient showed obvious retention of [^{11}C]BF-227 in the cerebellum, and lateral and medial temporal cortices. The three GSS patients showed significantly higher SUVRp in the lateral temporal cortex, thalamus and cerebellum (Table 1, Fig. 4) when compared to aged normal controls. Furthermore, when compared to the AD group, the GSS group showed significant elevation of SUVRp in the medial temporal cortex, thalamus and cerebellum. Although two GSS patients (GSS1 and GSS2) showed retention of BF-227 in most brain regions, the youngest GSS patient (GSS3) showed BF-227 retention only in the cerebellum, thalamus and medial temporal cortex, but not in the neocortex (Table 1, Fig. 4). Furthermore, two sporadic CJD patients showed no obvious BF-227 retention in any of the brain regions examined (Table 1, Fig. 4). As previously described [12, 21], AD patients showed [^{11}C]BF-227 retention in the neocortex; however, the cerebellum and medial temporal cortex were relatively spared (Table 1).

Autopsy examination of the brain of one GSS patient (GSS1) confirmed both the presence of abundant PrP amyloid plaques in the neocortex, cerebellum, basal ganglia, thalamus, entorhinal cortex and hippocampus and the absence of Aβ amyloid plaques or other structures of misfolded protein deposition such as Lewy bodies and neurofibrillary tangles. When compared to controls, the highest SUVRp percentage difference was found in the neocortex, especially in the frontal cortex (22%), followed by the striatum (12%), thalamus (9%), cerebellum (6%) and medial temporal cortex (3%) in this case. This finding was consistent with the autopsy result showing higher density of PrP amyloid plaques in the neocortex and basal ganglia than in the cerebellum, thalamus and hippocampus. Details of clinicopathological features of this case will be published elsewhere.

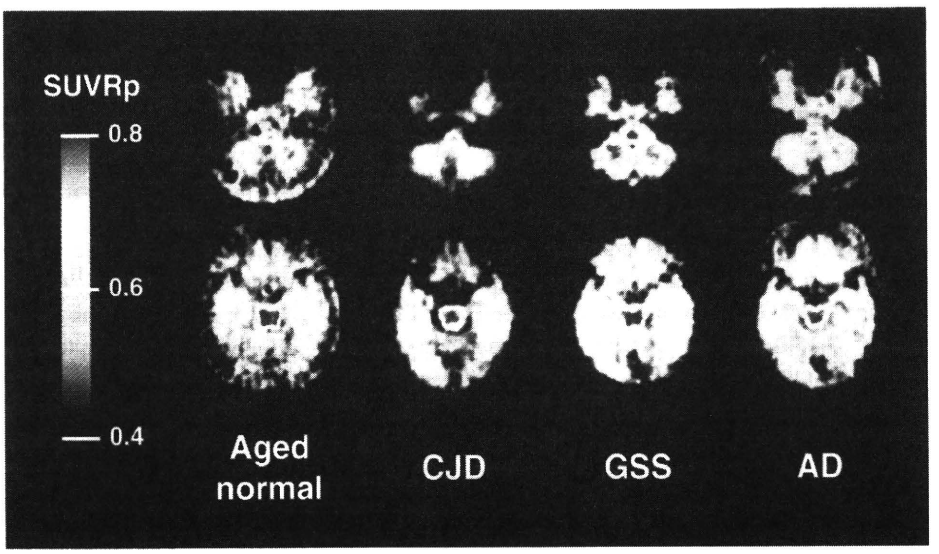

Fig. 3 Mean regional to pons standardized uptake value ratio (SUVRp) images between 40 and 60 min post-injection of [^{11}C]BF-227 in an aged normal subject (64-year-old man), a sporadic CJD patient (CJD1, 63-year-old woman), a GSS patient (GSS2, 61-year-old man) and an AD patient (62-year-old woman). Compared to the aged normal subject and CJD patient, the GSS patient showed obvious [^{11}C]BF-227 retention in the cerebellum and temporal cortex. The AD patient also showed obvious [^{11}C]BF-227 retention in the temporal cortex; however, the cerebellum was relatively spared

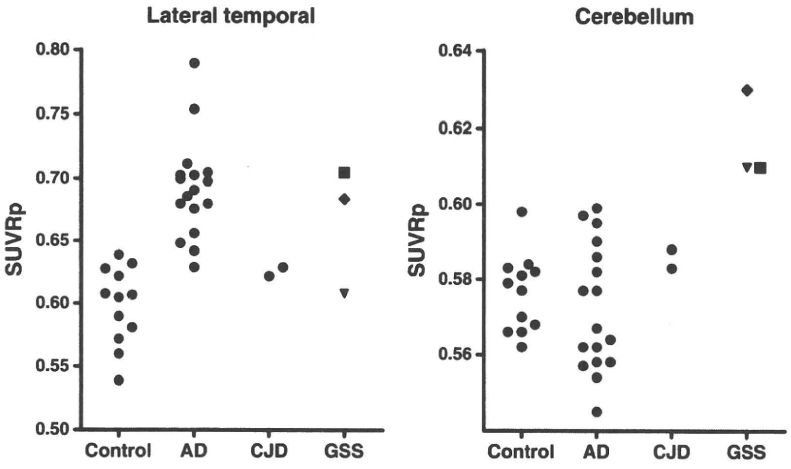

Fig. 4 SUVRp distribution in aged normal controls (*Control*), AD patients (*AD*), CJD patients (*CJD*) and GSS patients (*GSS*). GSS patients showed higher SUVRp values in the lateral temporal cortex and cerebellum. *Filled square* GSS1, *filled diamond* GSS2, *filled inverted triangle* GSS3

Discussion

This is the first study to demonstrate non-invasive detection of PrP amyloid plaques in GSS patients. GSS is neuropathologically characterized by deposits of multicentric amyloid plaques, which are especially abundant in the cerebellum, cerebral cortex and basal ganglia [3]. The present study demonstrated binding of BF-227 to PrP amyloid plaques in GSS brain sections. [^{11}C]BF-227 retention was observed in cortical and subcortical brain regions of GSS patients known for the high density of PrP plaques. Based on these findings, [^{11}C]BF-227 represents a promising candidate PET probe for the non-invasive detection of PrP amyloid plaques in the brain. However, the possibility that neocortical elevation of SUVRp in GSS patients might be caused by concomitant Aβ amyloid deposits or other misfolded protein deposits also should be considered, given that the two GSS patients showing prominent neocortical retention of [^{11}C]BF-227 were relatively older than the GSS patient showing no neocortical retention of BF-227. Although one positive GSS patient (GSS2) is still alive and was not examined neuropathologically, another positive case (GSS1) showed a high level of PrP amyloid deposits but no obvious deposits of Aβ amyloid or other misfolded proteins at autopsy. Furthermore, significant elevation of SUVRp was detected in the cerebellum, thalamus and hippocampus of all GSS cases. These brain regions are known to contain lower densities of Aβ plaques or other misfolded protein structures such as Lewy bodies. Based on these findings, it seems unlikely that concomitant deposition of Aβ amyloid or other misfolded proteins contributes to the high [^{11}C]BF-227 retention in GSS patients.

There is an increasing demand for in vivo detection of abnormal PrP deposition in the brain for the diagnosis of TSEs that might translate in early therapeutic intervention. Although GSS and other familial forms of TSEs can be diagnosed with PrP gene analysis using peripheral blood cells, it has been impossible to non-invasively measure the amount of abnormal PrP deposition in the brain. In a fashion similar to GSS, PrP amyloid deposition in the brain is commonly present in vCJD in which PrP amyloid plaques, called florid plaques, are pathognomonic [27]. Thus, [^{11}C]BF-227 PET might be a sensitive probe for the detection of PrP amyloid plaque deposition in vCJD as well as GSS, allowing longitudinal monitoring of PrP amyloid plaque deposition in the brain. Ante-mortem diagnosis of vCJD relies on the detection of abnormal PrP deposition in tonsil biopsy samples [28]. However, functional imaging using PET has an advantage over surgical biopsy tests in terms of both a non-invasive and an infection risk management point of view.

GSS is a rare form of TSE occurring in only about 3% of TSE cases in Japan. However, GSS is probably one of the TSEs most likely to benefit from early therapeutic interventions because the disease can be confirmed earlier using PrP gene analysis and progression occurs much more slowly than that in sporadic CJD, which comprises the majority of TSE cases. Recently, compounds such as pentosan polysulphate and doxycycline have been clinically used for experimental treatments for TSEs to prevent deposition of abnormal PrP in the brain, because these compounds slowed the disease progression in animal disease models when administered in an earlier stage of the disease [29–33]. Reliable surrogate markers are also required to evaluate the efficacy of these experimental interventions, and [^{11}C]BF-227 PET might be one of the best candidates to assess PrP amyloid deposition in GSS. However, it remains to be elucidated if PrP amyloid levels are a particularly relevant marker of therapeutic efficacy.

A previous PET study demonstrated moderate FDDNP retention and no remarkable PIB retention in the brain of two familial CJD patients with an octapeptide repeat insertion mutation [17]. A recent PET study has additionally demonstrated no PIB retention in two autopsy-confirmed sporadic

CJD patients [18]. In contrast with these studies, the present study successfully demonstrated prominent [^{11}C]BF-227 retention in the brain of GSS patients. Differences between the previous and present findings might mainly reside in the amount and type of PrP amyloid deposits in the brain, where histopathological studies indicate higher density of PrP amyloid plaques in GSS than in familial CJD [1]. In the present study, the findings in two sporadic CJD patients showing no obvious [^{11}C]BF-227 retention in the brain additionally support this speculation. The difference may also be attributable to higher binding affinity of BF-227 to PrP amyloid cores compared to FDDNP and PIB. To clarify this, further in vitro studies comparing the binding affinities of different amyloid tracers to PrP plaques in TSE brain homogenates are needed.

The youngest GSS patient (GSS3) showed BF-227 retention in the cerebellum and thalamus but not in the neocortex. The clinical symptoms in this patient were consistent with the brain distribution of BF-227, with the patient presenting with severe gait disturbance and slurred speech resulting from cerebellar ataxia but no signs of cognitive impairment, suggesting a close relationship between PrP plaque deposition as measured by BF-227 and regional brain dysfunction. There are variations of clinical phenotypes in GSS [1, 3]. Such variations are yet to be explained; however, the pattern of regional PrP amyloid distribution might be one of the factors affecting clinical phenotypes of GSS. In vivo PrP amyloid imaging using [^{11}C]BF-227 or other PET tracers will clarify neuropathological aspects of clinical variations in GSS.

In summary, we confirmed binding of BF-227 to PrP plaques in vitro and in vivo. A clinical PET study using [^{11}C]BF-227 demonstrated in vivo detection of PrP amyloid plaques in GSS patients. This imaging technique provides a potential means of facilitating both early diagnosis and non-invasive disease monitoring of certain forms of TSEs because, despite a lack of selectivity for PrP, brain retention of BF-227 in GSS shows a distinct pattern of regional distribution than that usually observed in sporadic AD.

Acknowledgment We appreciate the assistance of Dr. S. Watanuki, Dr. M. Miyake and Dr. H. Takashima in the clinical PET studies. This study was supported in part by the Program for the Promotion of Fundamental Studies in Health Science of the NIBIO in Japan, Industrial Technology Research Grant Program of the NEDO in Japan, and Health and Labor Sciences Research Grants (Translational Research and Research on Measures for Intractable Diseases) from the Ministry of Health, Labor, and Welfare of Japan.

References

1. DeArmond SJ, Kretzschmar HA, Prusiner SB. Prion diseases. In: Graham DI, Lantos PL, editors. Greenfield's neuropathology, 7th ed. London: Hodder Arnold. p. 273–323.
2. Collins SJ, Lawson VA, Masters CL. Transmissible spongiform encephalopathies. Lancet 2004;363:51–61.
3. Collins S, McLean CA, Masters CL. Gerstmann-Sträussler-Scheinker syndrome, fatal familial insomnia, and kuru: a review of these less common human transmissible spongiform encephalopathies. J Clin Neurosci 2001;8:387–97.
4. Noguchi-Shinohara M, Hamaguchi T, Kitamoto T, Sato T, Nakamura Y, Mizusawa H, et al. Clinical features and diagnosis of dura mater graft associated Creutzfeldt Jakob disease. Neurology 2007;69:360–7.
5. Lasmézas CI, Deslys JP, Demaimay R, Adjou KT, Hauw JJ, Dormont D. Strain specific and common pathogenic events in murine models of scrapie and bovine spongiform encephalopathy. J Gen Virol 1996;77(Pt 7):1601–9.
6. Schulz-Schaeffer WJ, Tschöke S, Kranefuss N, Dröse W, Hause-Reitner D, Giese A, et al. The paraffin-embedded tissue blot detects PrP(Sc) early in the incubation time in prion diseases. Am J Pathol 2000;156:51–6.
7. Fraser JR. What is the basis of transmissible spongiform encephalopathy induced neurodegeneration and can it be repaired? Neuropathol Appl Neurobiol 2002;28:1–11.
8. Small GW, Kepe V, Ercoli LM, Siddarth P, Bookheimer SY, Miller KJ, et al. PET of brain amyloid and tau in mild cognitive impairment. N Engl J Med 2006;355:2652–63.
9. Klunk WE, Engler H, Nordberg A, Wang Y, Blomqvist G, Holt DP, et al. Imaging brain amyloid in Alzheimer's disease with Pittsburgh Compound-B. Ann Neurol 2004;55:306–19.
10. Verhoeff NP, Wilson AA, Takeshita S, Trop L, Hussey D, Singh K, et al. In-vivo imaging of Alzheimer disease beta-amyloid with [11C]SB-13 PET. Am J Geriatr Psychiatry 2004;12:584–95.
11. Rowe CC, Ackerman U, Browne W, Mulligan R, Pike KL, O'Keefe G, et al. Imaging of amyloid beta in Alzheimer's disease with 18F-BAY94–9172, a novel PET tracer: proof of mechanism. Lancet Neurol 2008;7:129–35.
12. Kudo Y, Okamura N, Furumoto S, Tashiro M, Furukawa K, Maruyama M, et al. 2-(2-[2-Dimethylaminothiazol-5-yl]ethenyl)-6-(2-[fluoro]ethoxy)benzoxazole: a novel PET agent for in vivo detection of dense amyloid plaques in Alzheimer's disease patients. J Nucl Med 2007;48:553–61.
13. Ishikawa K, Doh-ura K, Kudo Y, Nishida N, Murakami-Kubo I, Ando Y, et al. Amyloid imaging probes are useful for detection of prion plaques and treatment of transmissible spongiform encephalopathies. J Gen Virol 2004;85:1785–90.
14. Bresjanac M, Smid LM, Vovko TD, Petric A, Barrio JR, Popovic M. Molecular-imaging probe 2-(1-[6-[(2-fluoroethyl)(methyl) amino]-2-naphthyl]ethylidene) malononitrile labels prion plaques in vitro. J Neurosci 2003;23:8029–33.
15. Sadowski M, Pankiewicz J, Scholtzova H, Tsai J, Li Y, Carp RI, et al. Targeting prion amyloid deposits in vivo. J Neuropathol Exp Neurol 2004;63:775–84.
16. Hoefert VB, Aiken JM, McKenzie D, Johnson CJ. Labeling of the scrapie-associated prion protein in vitro and in vivo. Neurosci Lett 2004;371:176–80.
17. Boxer AL, Rabinovici GD, Kepe V, Goldman J, Furst AJ, Huang SC, et al. Amyloid imaging in distinguishing atypical prion disease from Alzheimer disease. Neurology 2007;69:283–90.
18. Villemagne VL, McLean CA, Reardon K, Boyd A, Lewis V, Klug G, et al. 11C-PiB PET studies in typical sporadic Creutzfeldt-Jakob disease. J Neurol Neurosurg Psychiatry 2009;80:998–1001. doi:10.1136/jnnp.2008.171496.
19. Okamura N, Suemoto T, Shimadzu H, Suzuki M, Shiomitsu T, Akatsu H, et al. Styrylbenzoxazole derivatives for in vivo imaging of amyloid plaques in the brain. J Neurosci 2004;24:2535–41.
20. Ishikawa K, Kudo Y, Nishida N, Suemoto T, Sawada T, Iwaki T, et al. Styrylbenzoazole derivatives for imaging of prion plaques and treatment of transmissible spongiform encephalopathies. J Neurochem 2006;99:198–205.

21. Waragai M, Okamura N, Furukawa K, Tashiro M, Furumoto S, Funaki Y, et al. Comparison study of amyloid PET and voxel-based morphometry analysis in mild cognitive impairment and Alzheimer's disease. J Neurol Sci 2009;285:100–8. doi:10.1016/j.jns.2009.06.005.
22. Okamura N, Furumoto S, Funaki Y, Suemoto T, Kato M, Ishikawa Y, et al. Binding and safety profile of novel benzoxazole derivative for in vivo imaging of amyloid deposits in Alzheimer's disease. Geriatr Gerontol Int 2007;7:393–400.
23. Zeidler M, Gibbs CJ Jr, Meslin F. WHO manual for strengthening diagnosis and surveillance of Creutzfeldt-Jakob disease. Geneva: World Health Organization; 1998. p. 47–51.
24. McKhann G, Drachman D, Folstein M, Katzman R, Price D, Stadlan EM. Clinical diagnosis of Alzheimer's disease: report of the NINCDS-ADRDA Work Group under the auspices of Department of Health and Human Services Task Force on Alzheimer's Disease. Neurology 1984;34:939–44.
25. Friston KJ, Holmes AP, Worsley KJ, Poline JP, Frith CD, Frackowiack RSJ. Statistical parametric maps in functional imaging: a general linear approach. Hum Brain Mapp 1995;2:189–210.
26. Masters CL, Gajdusek DC, Gibbs CJ Jr. Creutzfeldt-Jakob disease virus isolations from the Gerstmann-Sträussler syndrome with an analysis of the various forms of amyloid plaque deposition in the virus-induced spongiform encephalopathies. Brain 1981;104:559–88.
27. Ironside JW, McCardle L, Horsburgh A, Lim Z, Head MW. Pathological diagnosis of variant Creutzfeldt-Jakob disease. APMIS 2002;110:79–87.
28. Hill AF, Zeidler M, Ironside J, Collinge J. Diagnosis of new variant Creutzfeldt-Jakob disease by tonsil biopsy. Lancet 1997;349:99–100.
29. Doh-ura K, Ishikawa K, Murakami-Kubo I, Sasaki K, Mohri S, Race R, et al. Treatment of transmissible spongiform encephalopathy by intraventricular drug infusion in animal models. J Virol 2004;78:4999–5006.
30. Rainov NG, Tsuboi Y, Krolak-Salmon P, Vighetto A, Doh-Ura K. Experimental treatments for human transmissible spongiform encephalopathies: is there a role for pentosan polysulfate? Expert Opin Biol Ther 2007;7:713–26.
31. De Luigi A, Colombo L, Diomede L, Capobianco R, Mangieri M, Miccolo C, et al. The efficacy of tetracyclines in peripheral and intracerebral prion infection. PLoS One 2008;3:e1888.
32. Teruya K, Kawagoe K, Kimura T, Chen CJ, Sakasegawa Y, Doh-ura K. Amyloidophilic compounds for prion diseases. Infect Disord Drug Targets 2009;9:15–22.
33. Forloni G, Salmona M, Marcon G, Tagliavini F. Tetracyclines and prion infectivity. Infect Disord Drug Targets 2009;9:23–30.